



The nature of the microquasar Cygnus X-3

New multiwavelength observations

K. I. I. Koljonen¹, M. L. McCollough², D. C. Hannikainen¹, and O. Vilhu³

¹ TKK/Metsähovi Radio Telescope, Metsähovintie 114, FIN-02540 Kylmäla, Finland
e-mail: karrri@kurp.hut.fi

² Smithsonian Astrophysical Observatory, 60 Garden Street, Cambridge, MA 02138-1516, USA

³ Observatory, PO Box 14, FIN-00014 University of Helsinki, Finland

Abstract. Cygnus X-3 is a well-known microquasar that shows state changes, strong radio emission, hard X-ray/soft X-ray/radio correlations, and relativistic jets. In 2006 after a period of almost four years of quiescence Cyg X-3 transitioned into an active state which included extended quenched emission and several major radio flares (up to 14 Jy). We conducted a large international observing campaign during this activity and we present here some results of our analysis. In this proceedings we will discuss the X-ray spectrum of Cyg X-3 during the major radio flares. We concentrated on the well-established method of studying black hole binary systems known as hardness-intensity diagram (HID) and applied this to Cyg X-3 archival data. In addition, we performed a principal component analysis (PCA) to study the intrinsic variability of the source during a major flare decay. The ramifications of our findings will be discussed.

Key words. Accretion, accretion disks – Binaries: close – Jets – X-rays: binaries – X-rays: individual: Cygnus X-3 – X-rays: stars

1. Introduction

Cygnus X-3 is a well-known X-ray binary (XRB), located ~ 9 kpc (Predehl et al. 2000) in the plane of the Galaxy. Its discovery dates back to 1966 (Giacconi et al. 1967) but the nature of the system has remained a mystery despite extensive X-ray and radio observations throughout the years. Its X-ray (Parsignault et al. 1972) and infrared (Mason et al. 1986) emission show a very strong 4.8-hour orbital modulation, typical of low-mass X-ray binaries. However, infrared observations indicate

that its mass-donating companion is a Wolf-Rayet (WR) star (Keerkwijk et al. 1992), which makes it a high-mass X-ray binary. Also unlike most other XRBs, Cyg X-3 is relatively bright in the radio virtually all of the time and it undergoes giant radio outbursts with strong evidence of jet-like structures moving away at relativistic speeds (Molnar et al. 1988; Schalinski et al. 1995; Mioduszewski et al. 2001).

The nature of the compact object is not clear, but it is thought to be a black hole due to its spectral resemblance to other black hole XRB systems, such as GRS 1915+105 and XTE J1550-564 (see e.g. Szostek, Zdziarski &

Send offprint requests to: K. I. I. Koljonen

McCollough 2008; Hjalmarsdotter et al. 2009). Also there is no evidence of a neutron star system launching such massive radio outbursts (up to 20 Jy, Waltman et al. 1995) as observed from Cyg X-3. Cyg X-3 is a unique system in our Galaxy, but recent observations of two XRBs in IC 10 (Prestwich et al. 2007) and NGC 300 (Carpano et al. 2007), both containing a WR companion, show strong evidence of a black hole primary. It is also noteworthy that these systems may represent a crucial link towards the evolution of a double black hole binary.

The X-ray spectra of Cyg X-3 are notoriously complex. Basically, Cyg X-3 exhibits the canonical X-ray states, namely the high/soft and low/hard states. Various intermediate states have also been observed between these canonical ones. The classification of Cyg X-3 X-ray spectra can be found in Szostek & Zdziarski (2004) and Hjalmarsdotter et al. (2009). The X-ray states more or less resemble the X-ray states found in other black hole XRBs. However, in Cyg X-3, the strong radio emission is also classified into states of its own (Waltman et al. 1996; McCollough et al. 1999). Ultimately, it has been found that these X-ray and radio states can be implemented into a more unified picture presented in Szostek, Zdziarski & McCollough (2008): the radio/X-ray states.

The X-ray emission has been found to be linked to radio emission in Cyg X-3. McCollough et al. (1999) found out that during periods of flaring activity in the radio the hard X-ray (HXR) flux switches from an anti-correlation to a correlation with the radio. In particular, for major radio flares and the quenched radio emission (very low radio fluxes of 10–20 mJy) which precedes them the correlation is strong. On the other hand McCollough, Koljonen & Hannikainen (2009) have found that although on the whole the radio and HXR appear to be correlated, they do not peak simultaneously during major flaring, but the HXR lags by three days compared to the radio. The exact nature of this correlation and the three day lag are currently being investigated (Koljonen et al. 2009, in prep.). In addition, the HXR flux has been shown to anti-

correlate with the soft X-rays in both canonical X-ray states (McCollough et al. 1999).

2. Hardness-intensity diagram of Cyg X-3

An important tool for understanding the nature of transient black hole systems is the hardness-intensity diagram (HID, e.g. Fender, Belloni & Gallo 2004 and references therein). A typical black hole HID has a Q-type shape (Fender, Belloni & Gallo 2004, their Fig. 7). We have produced a HID for Cyg X-3 (Fig. 1, see also McCollough, Koljonen & Hannikainen 2009 and their Fig. 2) from archival *RXTE*/PCA data with simultaneous or nearly simultaneous radio observations from GBI 8.3 GHz (Waltman et al. 1994, 1995, 1996), Ryle 15 GHz (part of a monitoring program) and RATAN-600 11.2 GHz (Thruskin, Bursov & Nizhelskij 2008). At first glance the plot appears very similar to a black hole HID, but there are some very important differences:

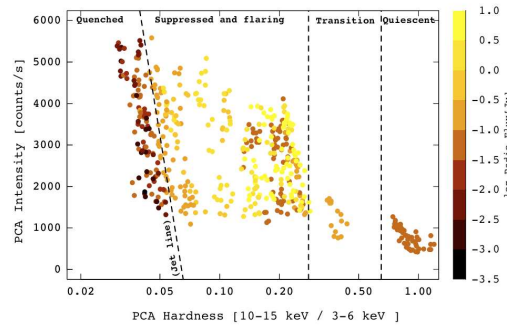


Fig. 1. The HID of Cyg X-3 with simultaneous or nearly simultaneous radio observations. The radio/X-ray states are marked according to the activity in the radio and X-ray hardness. See text for noted differences with black hole transient HID.

a) Cyg X-3 does not show hysteresis in the HID (as mentioned in Hjalmarsdotter et al. 2009), but simply increases the variability in the intensity as the spectra becomes softer; b) In the quiescent region Cyg X-3 is very bright in both the X-ray and the radio (60–200 mJy) compared to other black hole sys-

tems in this state. The X-ray spectrum in this state shows really strong iron lines and turns over at 20 keV, not at ~ 100 keV as seen in other black hole systems in the low/hard state (see e.g. Zdziarski 2009, these proceedings); c) There are two types of major flares present, corresponding to two vertical branches in the HID: major flares with HXR and without HXR. VLBI observations during the latter types of flares did not reveal any jet-like structure (Mioduszewski 2000, priv. comm.). These events possibly represent some type of “failed” jet (e.g. see simulations for the effect of stellar wind on the jet in Perucho & Bosch-Ramon 2008). Also, most remarkably, Cyg X-3 crosses the “jet line” from right to left (from minor flaring to quenching) without producing a major radio flare. It is only when it crosses from left to right that a major flare occurs.

3. New multiwavelength observations

In May–July 2006, an extensive international campaign was undertaken during and following three major radio flares (13.8 Jy and 7.9 Jy in the 15 GHz band for the double peaked first flare, 7.4 Jy in the 11.2 GHz band for the second flare and 1.8 Jy for the third flare). This included observations across the electromagnetic spectrum from three space-based (*INTEGRAL*, *Swift* and *RXTE*) and three ground-based observatories

(Ryle, RATAN-600 and PAIRITEL). The main blocks of observing time are centered shortly after the peak of each major flare, ranging from 0.25 days to 24.4 days after the flare. The lightcurves can be seen in Fig. 2. The *INTEGRAL* observations labeled Obs. 1 (MJD 53943), Obs. 2 (MJD 53868), Obs. 3 (MJD 53872), Obs. 4 (MJD 54014) and Obs. 5 (MJD 53966) are numbered according to the time elapsed since the peak of a major flare (see Table 1). In this proceedings we will concentrate mainly on the radio and *INTEGRAL* observations and refer the reader to Koljonen & McCollough (2009) and Koljonen et al. (2009, in prep.) for more complete coverage and data reduction of this multiwavelength campaign.

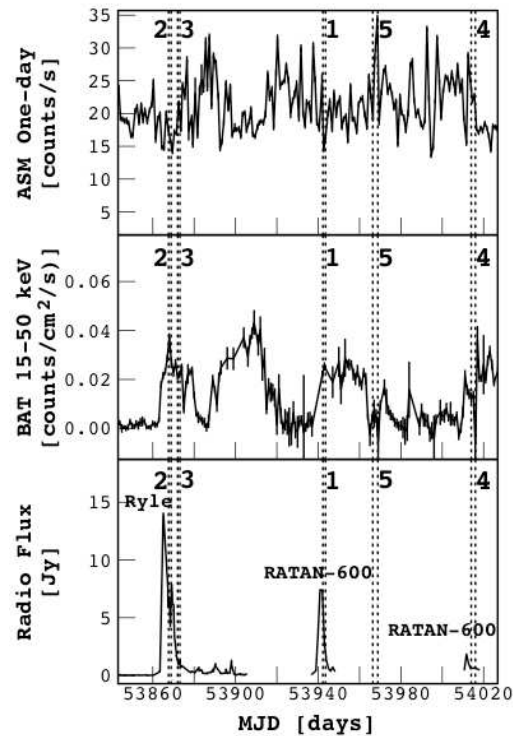


Fig. 2. Radio and X-ray coverage of the campaign spanning the three major flare events. From top to bottom: *RXTE*/*ASM* summed one-day averaged lightcurve (1.3–12.1 keV), *Swift*/*BAT* lightcurve (15–50 keV) and Ryle 15 GHz and RATAN-600 11.2 GHz fluxes. The epochs of the *INTEGRAL* observations are marked as vertical dotted lines and numbered according to the time elapsed since the peak of a major flare (see Table 1).

4. Principal component analysis

From the study by McCollough, Koljonen & Hannikainen (2009), the time evolution of the X-ray shows that they harden as the flare progresses. It appears that as the major radio flare fades there may be ongoing processes that are affecting the particle distribution which is associated with the production of the HXR. However, the variability within the observations was found to be rather constant. The spectral evolution appears to be slow, on timescales of days, but there are indications

Table 1. Time elapsed since the peak of the major flare. The whole length of the *INTEGRAL* observations are shown.

	Obs. 1	Obs. 2	Obs. 3	Obs. 4	Obs. 5
Time Since Peak [days]	0.25–1.50	2.51–3.74	2.89–3.99	2.31–4.33	24.4–26.8

that there may be short, abrupt hardening of the spectra. This may indicate that the HXR spectra evolve in a stochastic manner, which is expected if there are internal shocks within the jet which are giving rise to particle acceleration and modifying the particle distribution.

In order to study more thoroughly the variability of the spectra after a major flare event and subsequent flare decay, we performed a principal component analysis (PCA) to all of the individual spectra in all of our observations (i.e. Obs. 1–5) totaling 219 *INTEGRAL* spectra. We produced light curves in 15 energy bands out of each science window of *INTEGRAL/JEM-X* and *INTEGRAL/ISGRI* (exposure 20–30 min). We closely followed the work of Malzac et al. (2006) and the reader is highly recommended to read that paper and references therein for further details. The main use of PCA is to find the smallest number of components that are sufficient to explain the data losing the least amount of information in the process. Basically, PCA finds patterns in the data in a way that highlights the differences and similarities in the data set. In many-dimensional cases where a graphical representation is not convenient it is a particularly powerful analysis tool. By finding the “new coordinates” of the data set (i.e. the principal components) where the data points mainly cluster and disregarding the small scatter (most likely due to systematics and noise) that the data points have around these coordinates, the dimensionality of the data set is reduced greatly, and is defined only by these new coordinates.

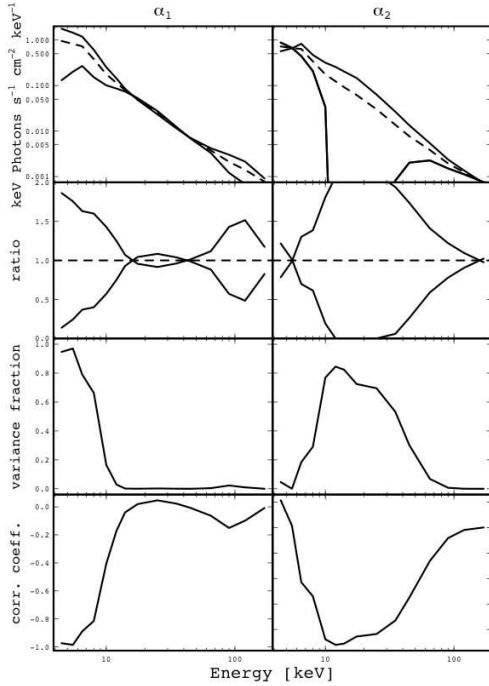


Fig. 3. The first two principal components (α_1 and α_2). The upper panels show the average (dash), minimum and maximum (thick lines) spectra of principal components. The upper middle panels show the ratio of minimum and maximum spectra to the average one. The lower middle panels shows the fraction of variance that the principal components explains in function of energy. The bottom panels show the correlation coefficients of the principal components with the flux in each energy band.

The result of the PCA is depicted in Figs. 3 and 4. Fig. 3 shows what is the effect of the two most significant principal components on the Cyg X-3 spectra and in what energy bands the variance occurs, as well as how it is correlated to the flux in each energy band. As can be seen from Fig. 3, the first component, contributing 86% of the overall variance, contributes to the change in normalization in the 4–10 keV band and it is (negatively) correlated with the orbital modulation. The second component, contributing 12% of the overall variance, contributes to the change in normalization in 10–50 keV

band and it is also correlated with the orbital modulation. The third component contributes only 1% and the rest of the components together less than 1% of the overall variance and is most likely due systematic errors and noise. Therefore we can say that the overall variability of the decaying major flare spectra is caused by two distinct components: say a disk in 4–10 keV band and a corona in 10–50 keV band, that are orbitally modulated with the system. Since they are modulated along with the fluxes, it means that the emission is local, compared to the radio flux that does not show any distinct modulation.

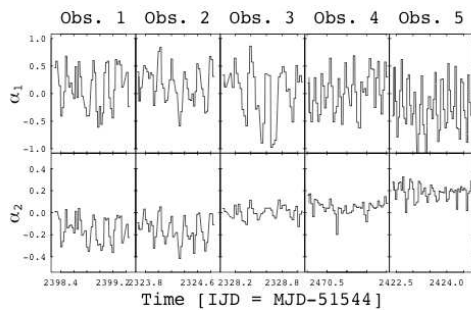


Fig. 4. The time variability of the two principal components in each observations. The 4.8 hour orbital modulation is clearly visible but it reduces in the second component as the flare progresses. See text for possible implications.

In Fig. 4 the evolution of the principal components are plotted. The observations are ordered again as the time since a major flare peak. The radio flux (not shown here) is not correlated to the principal components (Koljonen et al. 2009, in prep.) Note that the time axis of the last two panels from the left is twice as long as that of the first three. We can see that the first principal component oscillates around the same values and with same amplitudes throughout the decay. However, the second component shows time evolution as the range and amplitude change as the flare progresses. This ties in to the notion that the harder component is coupled to the decay process.

5. Discussion

The radio clearly plays a major role in determining the nature of Cyg X-3. In the quenched and major flaring states the HXR and radio are correlated, however the HXR lags ~ 3 days as compared to the radio data. In addition, there are two types of major radio flares: with HXR and without or very little HXR. The latter might be a consequence of a failed jet as the plasma fails to plow through the heavy stellar wind of the WR companion. The intrinsic variability of Cyg X-3 spectra during major flares and subsequent decay can be explained by two components: a low energy/disk component and a high energy/coronal component. Both components are orbitally modulated, so they are deep within the system. However, the second component shows a secular evolution as the flare progresses. The orbital modulation dampens, and it might be that if this component is due to an internal shock we see that the shock is moving out from the immediate vicinity of the compact object. Therefore this shock could Comptonize the soft electrons coming from the disk. The internal shock model to the radio flares of Cyg X-3 has been successfully implemented by Lindfors et al. (2007). Also the Cyg X-3 SEDs are well fitted with an absorbed thermal emission from the disk and a Comptonizing component supporting the two main components scenario (see Koljonen & McCollough 2009).

6. Conclusions

We have presented the main characteristics of Cyg X-3 and noted the complexity of the X-ray spectra and the tight interplay between the radio and X-rays in the source. We have investigated the HID of Cyg X-3 and it shows some similarity and some differences with black hole transient HIDs. When combined with the radio data, the radio/X-ray states are clearly revealed in the HID and we can see that the major flares in Cyg X-3 occur with variable X-ray hardness. We have also presented a more thorough study of the variability of X-ray spectra during major flares using principal component analysis. The results show that the variability in the spectra

can be explained by two components: an orbitally modulated soft component, presumably the accretion disk and a hard component which shows diminishing modulation. This might imply that the hard component is due to an internal shock and we see that the shock is moving out from the immediate vicinity of the compact object.

7. DISCUSSION

ANDRZEJ ZDZIARSKI: Is there any peculiarity in the 2007 radio outburst from which AGILE claimed GeV emission detection?

KARRI KOLJONEN: We just have analyzed the 2006 data set, so I can not comment anything on 2007 data.

JAMES BEALL: Say again what the delay is between the radio and the X-ray fluxes. And are there any quiescent periods you have observed?

KARRI KOLJONEN: Three days. Yes, we do have multiwavelength observations from quiescent period. The analysis is on-going.

Acknowledgements. We thank Sergei Trushkin for providing the RATAN-600 data and Guy Pooley for providing the Ryle data. KIIK gratefully acknowledges a grant from Jenny ja Antti Wihurin säätiö and Academy of Finland grant (project num. 125189). MLM acknowledges support for this work from NASA under contracts NAS8-03060 (CXC) and NNX06AB94G (Integral). DCH acknowledges Academy of Finland project number 212656. This research has made use of data obtained from the High Energy Astrophysics Science Archive Research Center (HEASARC), provided by NASA's Goddard Space Flight Center.

References

Carpano S., et al. 2007, A&A, 461, L9

- Fender, R. P., Belloni, T. E., Gallo E., 2004, MNRAS, 355, 1105
- Giacconi R., Gorenstein P., Gursky H., Waters J. R., 1967, ApJ, 148, L119
- Hjalmarsdotter L., et al. 2009, MNRAS, 392, 251
- Koljonen K. I. I. & McCollough M. L., 2009, in proceedings of 7th INTEGRAL Workshop, PoS(Integral08)075
- Koljonen K. I. I. et al., 2009, MNRAS, in preparation
- Lindfors E. J., et al. 2007, A&A, 473, 923
- Malzac, J., et al. 2006, A&A, 448, 1125-1137
- Mason, K.O., et al. 1986, ApJ, 309, 700
- McCollough, M., et al. 1999, ApJ, 517, 951
- McCollough, M. L., Koljonen K. I. I. & Hannikainen D. C., 2009, in proceedings of 7th INTEGRAL Workshop, PoS(Integral08)090
- Mioduszewski, A. J., 2000, private communication
- Mioduszewski, A. J. et al. 2001, ApJ, 553, 766
- Molnar, L.A., et al. 1988, ApJ, 331, 494
- Parsignault, D., et al. 1972, NaturePhys. Sci., 239, 123
- Perucho, M. & Bosch-Ramon, V, 2008, A&A 482, 917
- Predehl P., Burwitz V., Paerels F. & Trümper J., 2000, A&A, 357, L25
- Prestwich A. H., et al., 2007, ApJ, 669, L21
- Schalinski, C.J. et al, 1995, ApJ, 447, 752
- Szostek A. & Zdziarski A. A., 2004, arXiv:astro-ph/0401265
- Szostek A., Zdziarski, A. & McCollough, M. 2008, MNRAS, 388, 100
- Trushkin S. A., Bursov N. N. & Nizhelskij N. A., 2008, AIPC, 1053, 219T
- van Keerkwijk M. H., et al., 1992, Nature, 355, 703
- Waltman E. B., et al. 1994, AJ, 108, 179
- Waltman, E. B., et al. 1995, AJ, 110, 290
- Waltman E. B., et al. 1996, AJ, 112, 2690
- Zdziarski, A. A., 2009, these proceedings